

ORNL/Sub/94-SS112/07

SUPPORT SERVICES FOR CERAMIC FIBER-CERAMIC MATRIX COMPOSITES

Final Annual Technical Progress Report

November 2002

Report Prepared by
John P. Hurley and Patricia L. Kleven
Energy & Environmental Research Center
University of North Dakota
PO Box 9018
Grand Forks, North Dakota 58202-9018
under
Subcontract No. 19X-SS112V

for

OAK RIDGE NATIONAL LABORATORY
Oak Ridge, Tennessee 37831
Managed by
UT-BATTELLE, LLC
for the
U.S. DEPARTMENT OF ENERGY
Contract No. DE-AC05-96OR22464

This report has been reproduced directly from the best available copy.

Available to DOE and DOE contractors from the Office of Scientific and Technical Information, P.O. Box 62, Oak Ridge, TN 37831; prices available from (865) 576-8401.

Available to the public from the National Technical Information Service, U.S. Department of Commerce, 5285 Port Royal Rd., Springfield, VA 22161.

This report was prepared as an account of work sponsored by an agency of the United States Government. Neither the United States Government nor any agency thereof, nor any of their employees, makes any warranty, expressed or implied, or assumes any legal liability or responsibility for the accuracy, completeness, or usefulness of any information, apparatus, product, or process disclosed, or represents that its use would not infringe privately owned rights. Reference herein to any specific commercial product, process, or service by trade name, trademark, manufacturer, or otherwise, does not necessarily constitute or imply its endorsement, recommendation, or favoring by the United States Government or any agency thereof. The views and opinions of authors expressed herein do not necessarily state or reflect those of the United States Government or any agency thereof.

ORNL/Sub/94-SS112/07

SUPPORT SERVICES FOR CERAMIC FIBER-CERAMIC MATRIX COMPOSITES

Final Annual Technical Progress Report

November 2002

**Research sponsored by the U.S. Department of Energy
Office of Fossil Energy
Advanced Research Materials Program
DOE/FE AA 15 10 100
Work Breakdown Structure Element UNDEERC-4**

**Report Prepared by
John P. Hurley and Patricia L. Kleven
Energy & Environmental Research Center
University of North Dakota
PO Box 9018
Grand Forks, North Dakota 58202-9018
under
Subcontract No. 19X-SS112V**

for

**OAK RIDGE NATIONAL LABORATORY
Oak Ridge, Tennessee 37831
Managed by
UT-BATTELLE, LLC
for the
U.S. DEPARTMENT OF ENERGY
Contract No. DE-AC05-96OR22464**

LIST OF FIGURES

1	The EERC SPS 2
2	TRDU and HGFV in the EERC gasification tower 4
3	ORNL Cr-Ta coupons after removal from the SFS 9
4	Example of cross-sectioned alloy, corrosion product, and ash deposit at 100x magnification 10
5	Sample surface at 1500x magnification 11
6	ORNL Cr35-Fe coupons after removal from the SFS 12
7	Cross section of alloy showing corrosion and ash deposit at 100x 12
8	Sample surface at 1500x magnification 13
9	ORNL Cr6-MgO coupon after removal from the SFS ..	. 14
10	Cross section of alloy at 100x magnification 15
11	Alloy, oxide layer, and ash deposit at 1500x magnification 16

LIST OF TABLES

1	Composition of the Bulk Illinois No. 6 Coal Ash and the Convective Pass Deposits 6
2	Composition, Size, and Abundance of Minerals Present in Illinois No. 6 Coal 7
3	Mineral Phases and Frequency Present in Ash Deposits 8

SUPPORT SERVICES FOR CERAMIC FIBER-CERAMIC MATRIX COMPOSITES

Research sponsored by the U.S. Department of Energy, Fossil Energy Advanced Research Materials Program, DOE/FE AA 15 10 100, Work Breakdown Structure Element UNDEERC-4

INTRODUCTION

To increase national energy self-sufficiency for the near future, power systems will be required to fire low-grade fuels more efficiently than is currently possible. The typical coal-fired steam cycle used at present is limited to a maximum steam temperature of 540°C and a conversion efficiency of 35%. Higher working-fluid temperatures are required to boost efficiency, exposing subsystems to very corrosive conditions. In order to initially evaluate the suitability of a new material for use in a fossil energy system and to determine appropriate alterations in material composition or processing during the development stage, short-term tests of the corrosion resistance of the material and the corrosion mechanisms must be performed.

The University of North Dakota Energy & Environmental Research Center (EERC) is working with the Oak Ridge National Laboratory and the U.S. Department of Energy (DOE) National Energy Technology Laboratory to provide technical assistance and products of coal utilization to the Fossil Energy Materials Program investigating materials failure due to corrosion in fossil energy systems. The main activities of the EERC are to assemble coal slag and ash samples for use in corrosion tests by materials researchers, to assist in providing opportunities for realistic corrosion tests of advanced materials in pilot-scale fossil energy systems, and to provide analytical support in determining corrosion mechanisms of the exposed materials.

This work serves DOE goals of advancing the efficiency and reducing the emissions of coal-fired power plants by providing inexpensive and rapid initial tests of the corrosion resistance of newly developed advanced materials. The information is most useful in the development stage so that the potential of the material for use in a fossil energy system can be quickly assessed and so that modifications can be made to the material or its processing in order to increase its corrosion resistance. Upon successful testing under this program, the materials developer will be able to produce a more corrosion-resistant material, recommend appropriate uses for the material in a fossil energy system, and choose appropriate long-term testing scenarios under other programs.

In this report, we present the results of investigations by the EERC from October 2001 to September 2002. The two main pilot-scale power plant simulation systems at the EERC that can be used by researchers for realistic testing of materials are described. Researchers can include sample coupons in each of these facilities at no cost since they are being operated under separate funding. In addition, a pilot-scale coal combustion test is described in which material sample coupons were included. The results of scanning electron microscopy (SEM) energy-dispersive x-ray analyses of the corrosion products and interactions between the surface scales of the coupons and the products of coal combustion found on the coupons exposed during those tests are reported.

DESCRIPTIONS OF EERC PILOT-SCALE EQUIPMENT

Two pilot-scale solid fuel-fired test systems are being operated at the EERC in which materials coupons can be included for corrosion testing. The slagging furnace system (SFS) simulates the conditions in a commercial pulverized-fuel-fired combustion (oxidizing) system. Material coupons can be placed in zones exposed to gas and molten slag or fly ash at temperatures of approximately 1400°, 980°, or 750°C. The transport reactor development unit (TRDU) simulates the conditions in a commercial entrained-bed gasification (reducing) system. Coupons can be exposed in this system either on the clean or dusty side of a hot-gas filter operating at approximately 530°C.

Slagging Furnace System

Figure 1 is a simplified illustration of the SFS. It was constructed with funding from the DOE Combustion 2000 Program through a subcontract to the United Technologies Research Center to support testing and development of subsystems to be used in a high-temperature advanced furnace. The illustration consists of eight main components: 1) slagging furnace, 2) slag screen/slag tap, 3) dilution-quench zone, 4) process air preheaters, 5) convective air heater (CAH) section, 6) radiant air heater (RAH) panel, 7) tube-and-shell heat exchangers, and 8) pulse-jet baghouse. The SFS design is intended to be as fuel-flexible as possible, with maximum furnace exit temperatures of 1480° to 1590°C to maintain the desired heat transfer to the RAH panel and slag flow. The furnace has a nominal firing rate of 2.6×10^6 kJ/hr and a range of 2.1 to 3.2×10^6 kJ/hr using a single burner. The furnace design was based on Illinois No. 6

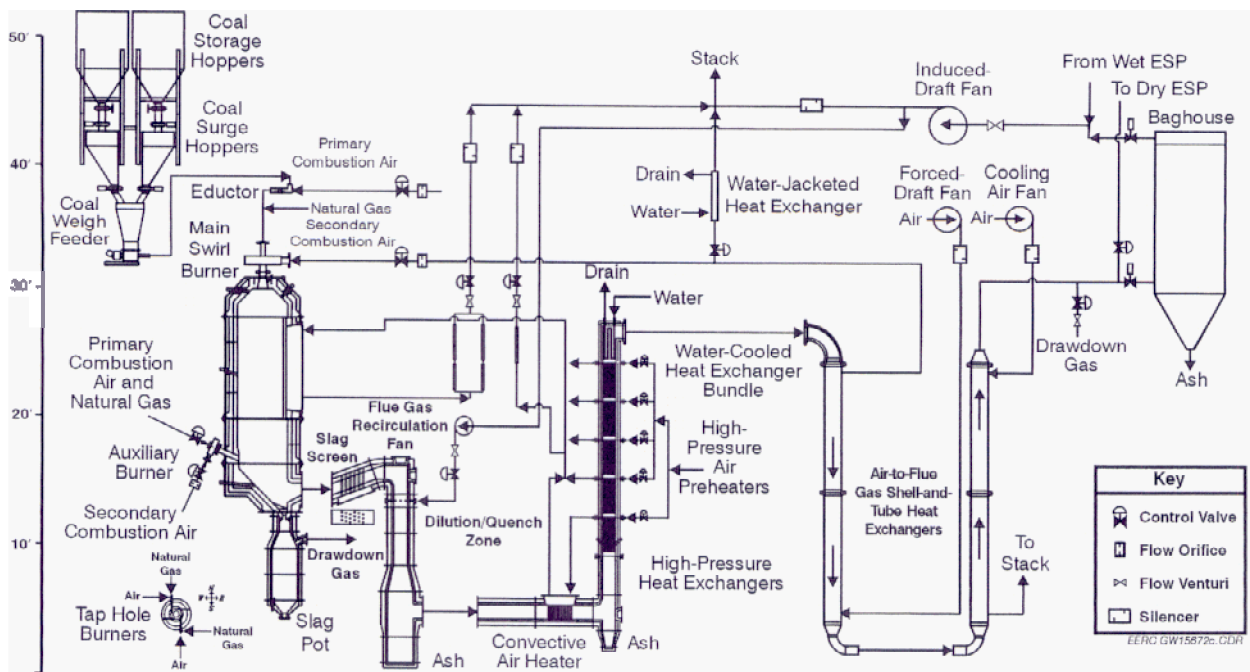


Figure 1. The EERC SFS.

bituminous coal (25,800 kJ/kg) and a nominal furnace residence time of 3.5 s. The EERC oriented the furnace vertically (downfired) so that slag would not interfere with the operation of the burner. Internal dimensions are 119 cm in diameter by roughly 4.9 m in total length. The SFS is lined with three layers of refractory totaling 30 cm thick to minimize heat loss. This insulation keeps the wall surface temperature near that of the gas stream. The inner layer is composed of an alumina castable, developed by the EERC in cooperation with the Plibrico Company, that has been shown in bench and pilot tests to be extremely resistant to slag corrosion at high wall temperatures.

Material sample coupons can be inserted into the system through ports in the main combustor, in the slag screen, or on racks in the convective pass downstream of the CAH. Most samples were included downstream of the CAH. Near that subsystem, gas temperatures are maintained at 980°C, but they drop farther back in the system to approximately 175°C as the gas enters the exit stack. To be included in SFS tests, materials coupons should be no more than 5 cm wide and able to be slipped onto a 1.2-cm-thick Inconel support rod.

Transport Reactor Development Unit

In addition to exposure to combustion conditions in the SFS, material coupons can also be exposed to gasification gas and dust in the hot-gas filter vessel (HGFV) of the TRDU. The TRDU is a 2.6×10^6 -kJ/hr pressurized circulating fluid-bed gasifier similar to the gasifier being tested at the Southern Company Services Wilsonville, Alabama, facility. The system is illustrated in Figure 2. It has an exit gas temperature of up to 980°C, a nominal gas flow rate of 5×10^3 m³/hr, and an operating pressure of 0.93–1.1 MPa. The TRDU system can be divided into three sections: the coal feed section, the TRDU, and the product recovery section. The TRDU proper consists of a riser reactor with an expanded mixing zone at the bottom, a disengager, and a primary cyclone and standpipe. All of the components in the system are refractory-lined and designed mechanically for 1.1 MPa and an internal temperature of 1090°C.

The premixed coal and limestone fed to the transport reactor can be admitted through one of three nozzles that are at varying elevations. Oxidant is fed to the reactor through two pairs of nozzles at varying elevations within the mixing zone. For the combustion mode of operation, additional nozzles are provided in the riser for feeding secondary air. Hot solids from the standpipe are circulated into the mixing zone, where they come into contact with the oxidant and the steam, which is injected into the J-leg. This feature enables spent char to contact oxidant and steam prior to the fresh coal feed. Gasification or combustion and desulfurization reactions are carried out in the riser, as coal, sorbent, and oxidant (with steam for gasification) flow up the riser. The solids circulation into the mixing zone is controlled by the solids level in the standpipe. The bulk of entrained solids leaving the riser is separated from the gas stream in the disengager and circulated back to the riser via the standpipe. A solids stream is withdrawn from the standpipe via an auger to maintain the system's solids inventory at an appropriate level. Gas exiting the disengager enters a primary cyclone that has been modified to provide variable particulate collection performance. Solids from the dipleg of the primary cyclone are collected in a lock hopper. Gas exiting this cyclone enters a jacketed-pipe heat exchanger before entering the

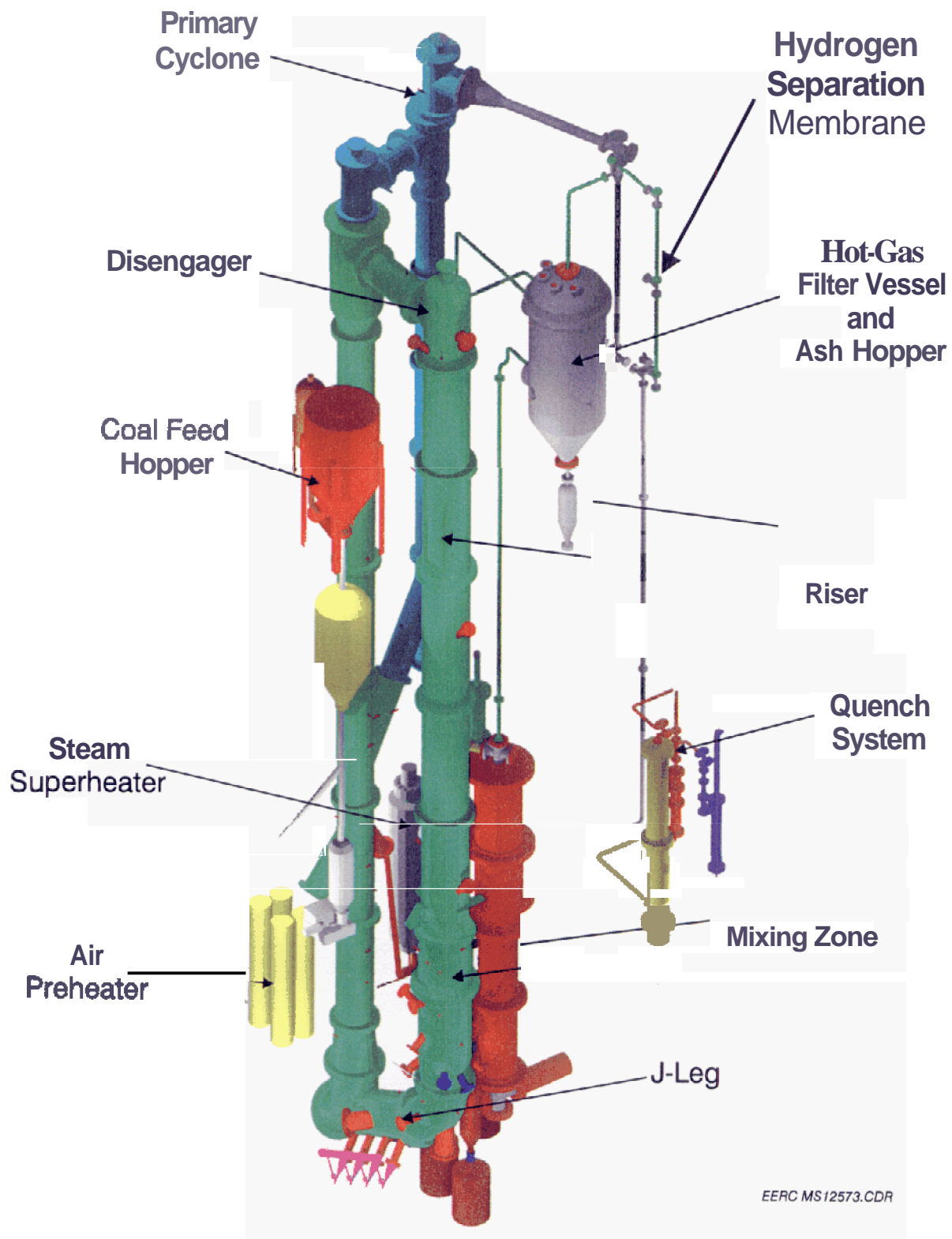


Figure 2. TRDU and HGFV in the EERC gasification tower.

HGFV at approximately 930°C. The cleaned gases leaving the HGFV enter a quench system before being depressurized and vented to a flare.

This vessel is designed to handle all of the gas flow from the TRDU at its expected operating conditions. The vessel is approximately 1.2 m inner diameter (i.d.) and 4.7 m long and is designed to handle gas flows of approximately 550 m³/hr at temperatures up to 980°C and 0.99 MPa. The refractory has a 0.71-m i.d. with a shroud diameter of approximately 0.56 m. The vessel is sized such that it could handle candle filters up to 1.5 m long; however, 1.0-m candles are being used in the initial 540°C gasification tests. Candle filters are 60 mm outer diameter with 10-cm center-to-center line spacing. The total number of candles that can be mounted in the current geometry of the HGFV tube sheet is 19.

Standard TRDU tests consist of 200 hours of operation under gasification conditions with the HGFV operating at temperatures of 540°–650°C, 0.93 MPa. Material coupons are exposed in the system by sliding them over 1.3-cm-diameter stainless steel rods in the free space below the candle filters. Samples up to 5.1 cm wide can be included. The composition of the gas to which the material coupons would be exposed in the HGFV is approximately 8%–14% H₂O, 6%–9% each of CO and H₂, 8%–10% CO₂, and 1.0%–2.5% CH₄, with the balance being N₂ and other trace constituents.

RESULTS AND DISCUSSION OF THE COUPON TESTING

The EERC performed a 100-hr test in the SFS in November of 2001, during which ceramic and alloy samples were exposed to coal combustion conditions. The samples included three alloy rings from Oak Ridge National Laboratory (ORNL), two of these containing chromium with iron, tantalum, molybdenum, titanium, and silicon. The remaining alloy contained chromium with magnesium oxide, tantalum, and lanthanum oxide. Ten alloy samples were also included from Applied Thin Films, Inc. (ATFI). These alloys included two disks and eight rectangular samples. The metal content and coating material of these alloys have not been disclosed. Nine alloy and ceramic samples were also reinstalled that had previously been exposed in March and June 2000 SFS tests. The samples included two SiC/SiC rings from Allied Signal Composites, Inc., four mullite rings from Honeywell Advanced Composites, Inc., and three chrome/tantalum alloy rings from ORNL. All samples were installed in the convective pass, where they were heated to an average temperature of 935°C while firing an Illinois No. 6 bituminous coal. Brownish-gray scales covered with thick ash deposits were observed on all samples. No visible signs of erosion or major corrosion were observed on any of the alloys or ceramic rings. One sample from each type of chrome/tantalum alloy received from ORNL was analyzed by SEM, which verified the absence of major corrosion or erosion. The remaining samples were returned to their prospective suppliers.

Ash Deposit Analyses

Samples of bulk coal ash and ash deposits formed in the vicinity of the samples in the convective pass were analyzed by wavelength-dispersive x-ray fluorescence (WDXRF) and SEM

point count (SEMPC), respectively. As shown in Table 1, the deposits that formed in the convective pass on the SFS coupons contained slightly more Ca than the bulk coal ash, but otherwise they have similar compositions. This is a relatively uncommon result since in most coals, certain mineral types tend to concentrate in larger or smaller size ranges. As the particles pass through the combustion system, they tend to become segregated by size, with the larger particles (> 10 microns) depositing preferentially in the slag screen and smaller ones passing through to deposit on downstream surfaces such as the coupons in the convective pass. Therefore, elements that make up the larger particles are often depleted in the ash deposits formed in the convective pass, and those that make up the smaller particles tend to enrich the ash deposits. Table 2, which shows computer-controlled SEM (CCSEM) analyses of the minerals in the coal, indicates that the mineral matter in the coal is composed primarily of silica-rich clays, partially oxidized iron sulfide listed as pyrrhotite, and mineral particles of mixed compositions. For this coal, the particles listed as mixed have compositions indicating that they are primarily aluminosilicate clay particles with some sulfur. The sulfur peak in the x-ray signal is most likely from organically associated sulfur in the carbonaceous material surrounding the clay particle, not actually part of the clay. The size distribution of the clays and mixed particles indicates that they are relatively small particles, and the iron-rich pyrrhotite particles are relatively large. The fact that there is no depletion of iron in the ash deposits indicates that the pyrrhotite particles fragmented upon combustion and so were not preferentially removed in the slag screen.

Table 1. Composition of the Bulk Illinois No. 6 Coal Ash and the Convective Pass Deposits, normalized sulfur-free oxide basis

Oxides, wt%	Illinois No. 6 Coal Ash	Convective Pass Ash Deposit
SiO ₂	52.4	50.9
Al ₂ O ₃	24.1	22.1
Fe ₂ O ₃	15.1	15.0
TiO ₂	1.1	1.5
P ₂ O ₅	0.1	0.1
CaO	2.9	6.2
MgO	1.7	1.4
Na ₂ O	0.3	0.4
	2.3	2.3
SO ₃	2.7	0.0

Table 3 shows the SEMPC data which indicate the relative volume percent of the deposits with the compositions indicated. The composition names were derived from mineral names, but do not necessarily indicate that the mineral type is actually present, just that a portion of the ash deposit has a composition similar to that of the named mineral. In fact, most of the deposit is likely to be amorphous rather than crystalline. The data show that the bulk of the deposit is aluminosilicate-rich material, most likely glassy phases formed from the interaction of the clays with the other minerals during combustion. Only a minority of the pyrrhotite remained separate from the glassy

Table 2. Composition, Size, and Abundance of Minerals Present in Illinois No. 6 Coal, wt% on a mineral basis

	1.0 to 2.2 mm	2.2 to 4.6 mm	4.6 to 10.0 mm	10.0 to 22.0 mm	22.0 to 46.0 mm	46.0 to 100 mm	Totals	% Excluded
Quartz	0.5	1.1	2.5	1.9	0.7	0.3	6.9	57.8
Iron Oxide	0.1	0.1	0.6	0.3	0.7	0.9	2.7	80.1
Periclase	0	0	0	0	0	0	0	0
Rutile	0	0	0	0	0	0	0	0
Alumina	0	0	0	0	0	0	0	0
Calcite	0	0	0.3	0.5	0.9	0.4	2.1	90.2
Dolomite	0	0	0	0.1	0	0	0.1	100.0
Ankerite	0	0	0	0	0.1	0	0.1	100.0
Kaolinite	1.1	2.6	2.9	2.4	0.6	0.5	10.1	53.1
Montmorillonite	0.4	0.5	0.6	0.7	0.2	0.2	2.7	41.4
K Al-Silicate	1.4	3.3	3.4	3.5	1.5	1.4	14.5	52.3
Fe Al-Silicate	0	0.2	0.2	0	0	0	0.4	45.5
Ca 4-Silicate	0	0	0	0	0	0	0	0
Na Al-Silicate	0	0	0	0	0	0	0	46.8
Aluminosilicate	0	0.1	0.2	0.1	0.1	0	0.4	80.1
Mixed Al-Silica	0	0.4	0.2	0	0.1	0.1	0.8	40.9
Fe Silicate	0	0	0	0	0	0	0	100.0
Ca Silicate	0	0	0	0	0	0	0	0
Ca Aluminate	0	0	0	0	0	0	0	0
Pyrite	0	0	0.1	0.5	0.5	0.3	1.4	56.0
Pyrrhotite	0.3	1.8	2.4	7.8	8.6	7.7	28.6	85.1
Oxidized Pyrrhotite	0.4	0.4	0.5	0.8	1.0	0.7	3.8	78.6
Gypsum	0	0.4	0.2	0	0	0	0.6	74.7
Barite	0	0	0	0	0	0	0	0
Apatite	0	0	0	0	0	0	0	0
Ca Al-P	0	0	0	0	0	0	0	0
KCl	0	0	0	0	0	0	0	0
Gypsum/Barite	0	0	0	0	0	0	0	0
Gypsum/Al- Silicate	0.1	0.1	0.1	0.2	0	0	0.4	81.6
Si-Rich	0.3	0.6	0.6	0.7	0.3	0	2.5	43.4
Ca-Rich	0	0	0	0.1	0	0	0.1	100.0
Ca-Si-Rich	0	0	0	0	0	0	0	0
Mixed	5.1	5.3	3.4	2.3	3.9	1.9	21.7	37.5
Totals	9.9	16.8	18.1	21.9	19.0	14.4	100.0	

phases, undergoing oxidation and ending up in the deposits as iron oxide particles. Essentially no sulfur is present in the ash deposits.

Additional SFS tests are scheduled in the coming 18 months. One test will be a purely coal-fired test, probably oxygen-blown combustion. The other tests are expected to include coal cofired with biomass.

Table 3. Mineral Phases and Frequency Present in Ash Deposits

Mineral Name	Frequency, %	Mineral Name	Frequency, %
Oxide-Rich		Silicon-Rich	
Magnesium Oxide	0	Quartz	4.7
Aluminum Oxide	0	Albite	0
Calcium Oxide	0	Anorthite	5.1
Titanium Oxide	0	Potassium Feldspar	0
Chromium Oxide	0	Nepheline	0
Iron Oxide	9.4	Hauyne	0
Spinel	0	Leucite	0
Ca, Ti Oxide	0	Kaolinite	0
Ca, Al Oxide	0	Altered Kaolinite	3.4
Mixed Oxide-Rich	0	Illite	12.3
Total for Group	9.4	Montmorillonite	1.7
Sulfur-Rich		Pyroxene	0
Pyrite	0	Wollastonite	0.4
Pyrrhotite	0	Ca Silicate	0
Iron Sulfate	0	Dicalcium Silicate	0
Sodium Sulfate	0	Na CaSiO ₃	0
Calcium Sulfate	0	Gehlenite	0
NaCa Sulfate	0	Akermanite	0
Barite	0	Merwinite	0
Mixed Sulfur-Rich	0.4	Spurrite	0
Total for Group	0.4	Mullite	0
Phosphorus-Rich		Mixed Silicon-Rich	57.4
Apatite	0	Total for group	85.1
Mixed Phosphorus-Rich	0	User-Defined List	
Total for Group	0	Halite	0
Carbon-Rich		AlSiCa1	0
Calcite	0	AlSiCa2	0
Altered Calcite	0	Total for Group	0
Dolomite	0	Other	1.3
Sulfated Dolomite	0		
Ankerite	0		
Sulfated Ankerite	0		
Mixed Carbon-Rich	3		
Total for Group	3		
Metal-Rich			
Aluminum	0		
Titanium	0		
Iron	0		
Nickel	0		
Copper	0		
Chromium	0		
Mixed Metal-Rich	0.9		
Total for Group	0.9		

Coupon Analysis Results

NMARL Sample 02-0451 Submitted by Mike Brady, ORNL Cr-Ta Alloy C

Sample Description

Shiny gray alloy ring, 12.5 mm high by 24 mm diameter, with a wall thickness of 6 mm.

Postexposure Appearance

Figure 3 shows the sample removed from the sample holder downstream of the CAH after the November 2001 test run. Flue gas flow across the alloy was from left to right. The ash deposit was easily removed from the alloy, leaving a thin coating of ash. What could be seen of the alloy surface was no longer shiny; it appeared dull dark gray and brown, with no flaking.

SEM Analysis

The alloy was reported to contain 82.75 wt% Cr, 9 wt% Ta, 5 wt% Mo, 3 wt% Si, 0.15 wt% La, and 0.1 wt% Ti. Figure 4 shows a representative example of the cross-sectioned coupon, corrosion product, and ash deposit at 100x magnification. It reveals a dual-phase field of alloy, a typical corrosive intrusion into the sample, and the thin discontinuous oxide layer coating the sample with ash above. A few large cracks were observed, which generally run parallel to the surface of the alloy, were randomly distributed about the sample, and extended several millimeters into the alloy.

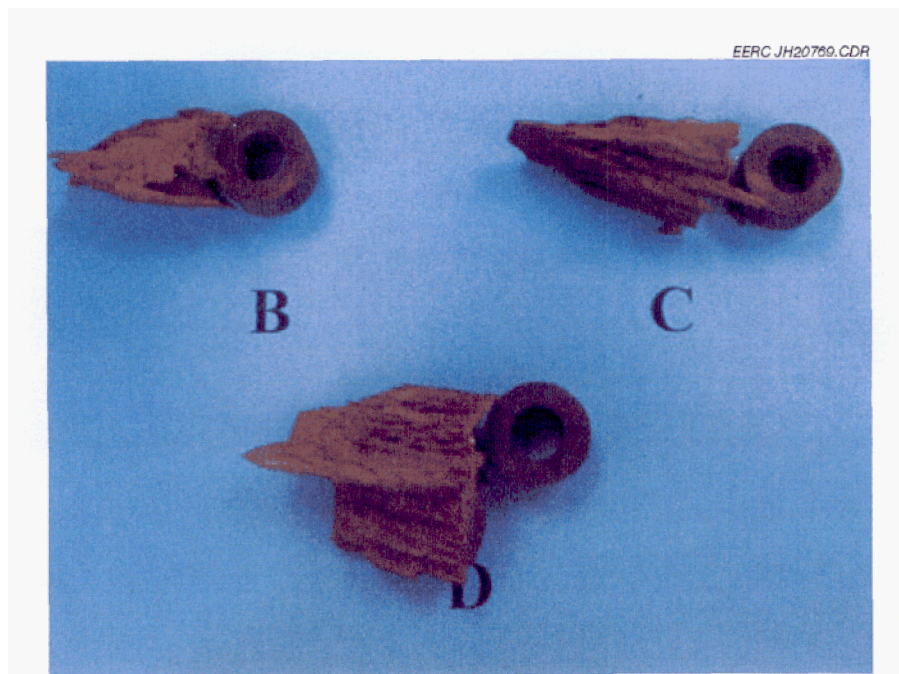


Figure 3. ORNL Cr-Ta coupons after removal from the SFS.

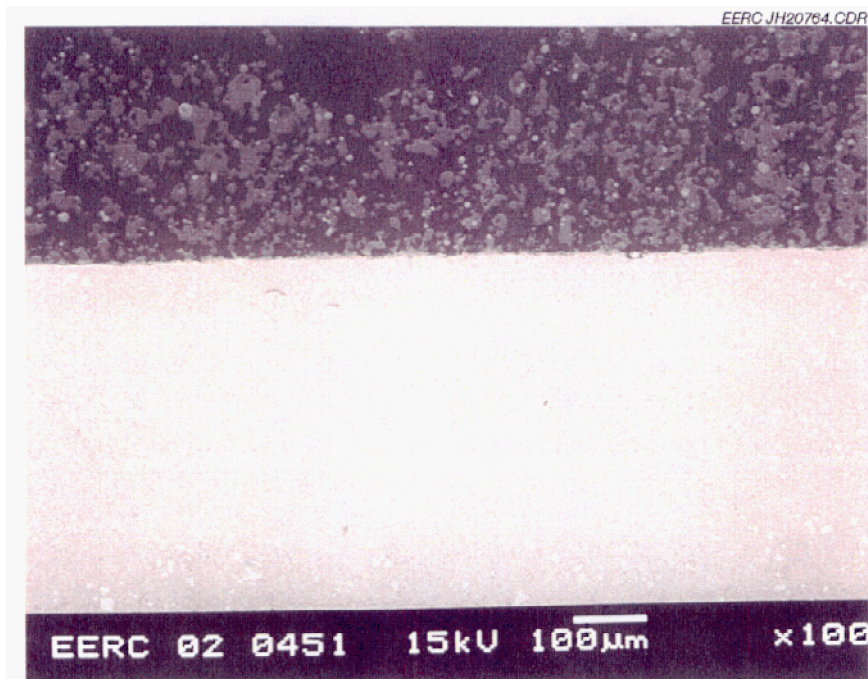


Figure 4. Example of cross-sectioned alloy, corrosion product, and ash deposit at 100x magnification (ORNL Cr-Ta Coupon C).

The alloy was composed of essentially a chromium matrix reinforced with a Cr-Ta intermetallic phase. A spot analysis of the matrix gave a composition of approximately 92 wt% Cr, 7 wt% Mo, 1 wt% Si, with an intermetallic composition of approximately 47 wt% Ta, 34 wt% Cr, 15 wt% Si, and 4 wt% Mo. The alloy near the surface appeared to be altered. The matrix was slightly enriched in molybdenum, silicon content doubled, and tantalum showed a fourfold increase below the oxide layer. In the same region, the intermetallic phase had a slight reduction in silicon, reduction by half of tantalum, and a threefold increase in molybdenum. Fine porosity was observed to a depth of approximately 15–20 μm . The diameter of the pores was less than 2 μm .

Figure 5 illustrates the discontinuous oxide layer with ash deposit attached at 1500x magnification. This figure also clearly shows the Cr-Ta intermetallic phase in a chromium matrix previously discussed. The oxide layer is essentially chromium oxide, which ranges from 2–4 μm in thickness, where present. The layer is enriched with silicon and tantalum at the alloy interface, but tantalum was not detected at the layer surface. However, near the surface, iron, calcium, and aluminum were detected, indicating that the oxide layer reacted with the ash. Chromium was detected in the ash material above the oxide layer in amounts as high as 13 wt%. The alloy surface, both covered with chromium oxide and uncovered, had a 2- μm -thick zone that was highly porous and broken. The corrosion mechanism appeared to be oxidation. Sulfidation, halide attack, or ash constituent interaction directly with the alloy was not detected.

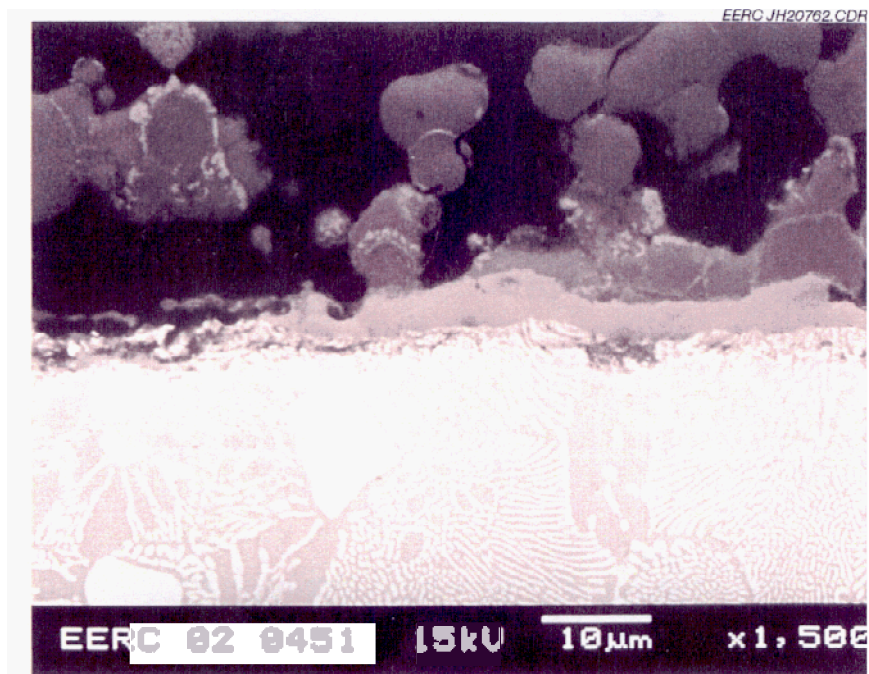


Figure 5. Sample surface at 1500x magnification (ORNL Cr-Ta Coupon C).

NMARL Sample 02-0452 Submitted by Mike Brady, ORNL Cr35-Fe Samples

Sample Description

Shiny gray alloy ring, 12.7 mm high by 24.9 mm diameter, with a wall thickness of 5.7 mm.

Postexposure Appearance

Figure 6 shows the samples removed from the sample holder downstream of the CAH after the November 2001 test run. Flue gas flow across the alloy was from left to right. The ash deposit separated easily from the alloy, leaving a thin coating of ash. The surface of the alloy was no longer shiny and appeared dark gray to brown, with no indications of flaking.

SEM Analysis

The reported composition of this alloy was 54.5 wt% Cr, 35 wt% Fe, 5.5 wt% Ta, 4 wt% Mo, 0.5 wt% Ti, and 0.3 wt% Si. A representative example of the cross-sectioned coupon at 100x magnification is shown in Figure 7. It reveals a dual-phase field of alloy, a typical corrosive intrusion into the sample, and the thin discontinuous poorly attached oxide layer coating the sample with ash above. Many areas showed the beginning of pit formation, and none was observed deeper than 10 µm.

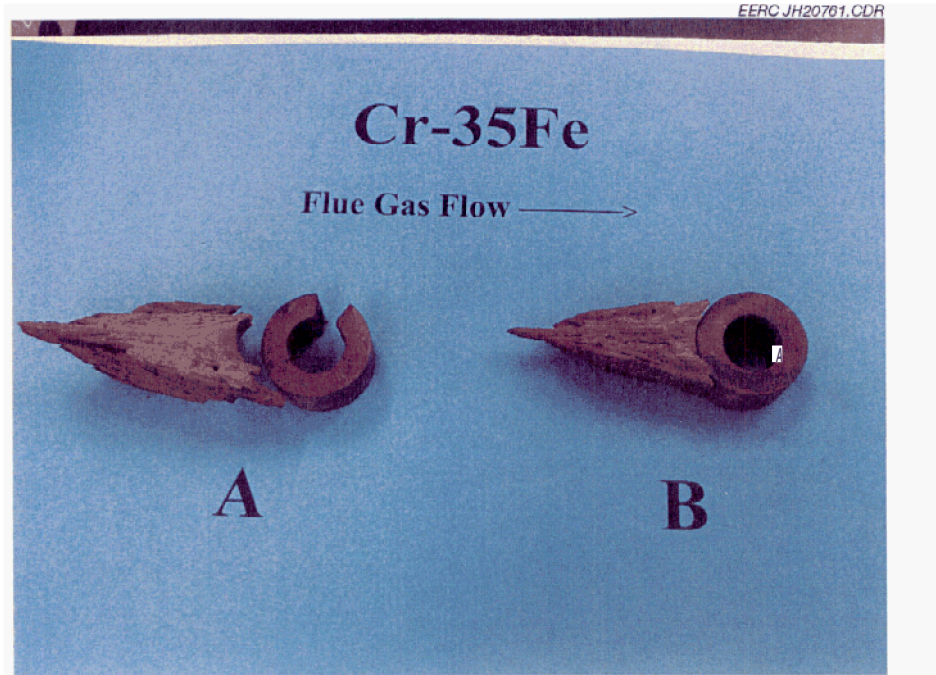


Figure 6. ORNL Cr35-Fe coupons after removal from the SFS.

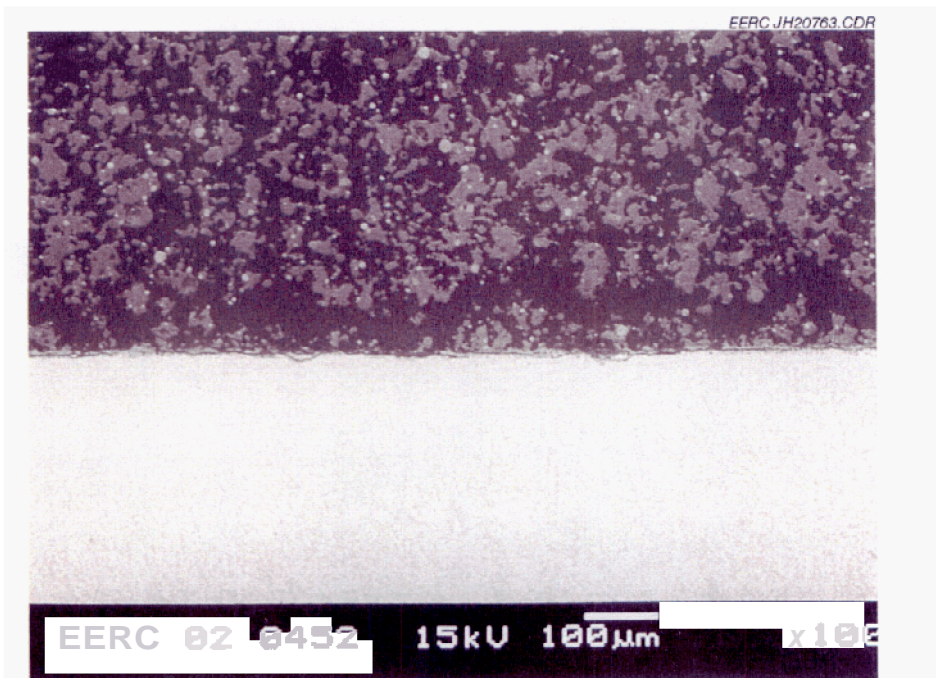


Figure 7. Cross section of alloy showing corrosion and ash deposit at 100x (ORNL Cr35-Fe Coupon A).

The matrix of the alloy was analyzed as having a composition of 62 wt% Cr, 34 wt% Fe, and 4 wt% Mo. Silicon and tantalum were found in trace amounts. The intermetallic phase was found to have a composition of 44 wt% Ta, 24 wt% Fe, 15 wt% Cr, 13 wt% Si, and 4 wt% Mo. Near the surface matrix, enrichment of iron, tantalum, molybdenum, and silicon was measured. Iron enrichment was only 6 wt% on average whereas the molybdenum content doubled, silicon had a threefold increase, and tantalum was found to have a fivefold increase, Chromium content decreased by 20 wt%. The intermetallic phase near the surface was measured to have a decrease by half of chromium, tantalum, and silicon, with only a slight increase in molybdenum.

The oxide layer was found to be chromium oxide with a few percent iron and silicon. Thickness was fairly uniform, where present, and was measured to be 5–7 μm thick. The top 5 μm of alloy at the oxide interface was highly porous and broken. Figure 8 illustrates the oxide layer, porous alloy, and ash at a magnification of 1500x. The oxide layer was found to have reacted significantly with the ash. The iron content of the oxide layer was greatest at the metal interface and the ash contact zone. Aluminum was measured at 2–3 wt% throughout the oxide layer. Chromium from the alloy was detected in the ash layer at approximately 2 wt%. Like the previous sample, oxidation was found to be the corrosion mechanism. Sulfidation, halide attack, or ash constituent interaction directly with the alloy was not detected.

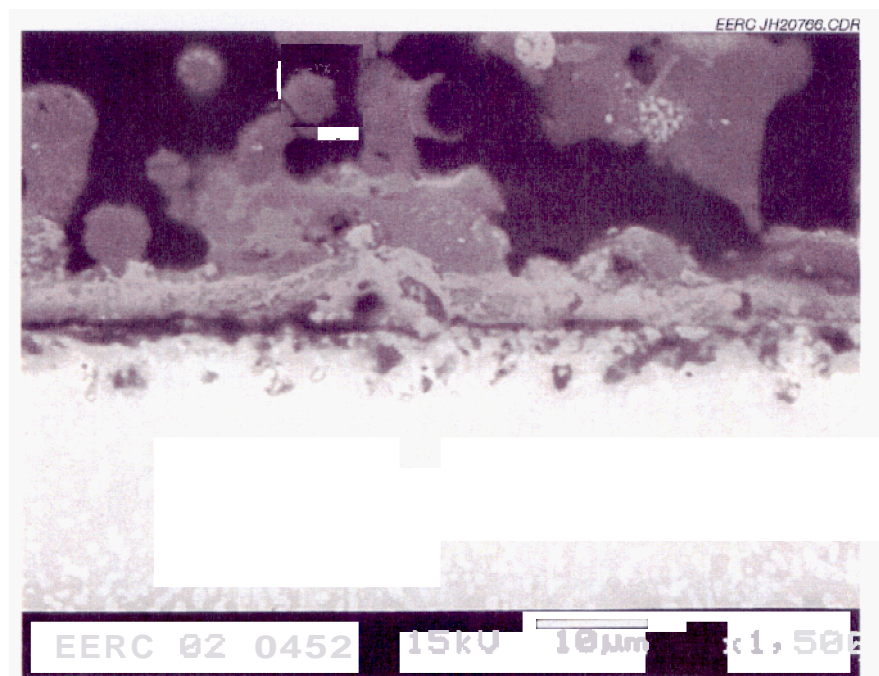


Figure 8. Sample surface at 1500x magnification (ORNL Cr35–Fe Coupon A).

NMARL Sample 02-0453 Submitted by Mike Brady, ORNL Cr6-MgO

Sample Description

Shiny gray alloy ring, 12.7 mm high by 25.4 mm diameter, with a wall thickness of 6.4 mm.

Postexposure Appearance

Figure 9 shows the sample removed from the holder downstream of the CAH after the November 2001 test run. Flue gas flow across the alloy was from left to right. As with the other two samples, the ash deposit was easily separated from the alloy, leaving a thin layer of ash. The alloy surface was no longer shiny. Instead, it appeared dull dark gray to brown, with no visible degradation or flaking of the surface.

SEM Analysis

Figure 10 shows a typical example of the cross-sectioned coupon at 100x. It reveals a triphase field of alloy, typical corrosion, a discontinuous oxide layer, and the ash above. The reported alloy composition was 93.2wt% Cr, 6 wt% MgO, 0.5 wt% Ti, and 0.3 wt% La₂O₃. Indications of pitting directly under the oxide layer were noted but no evidence of cracking was observed.

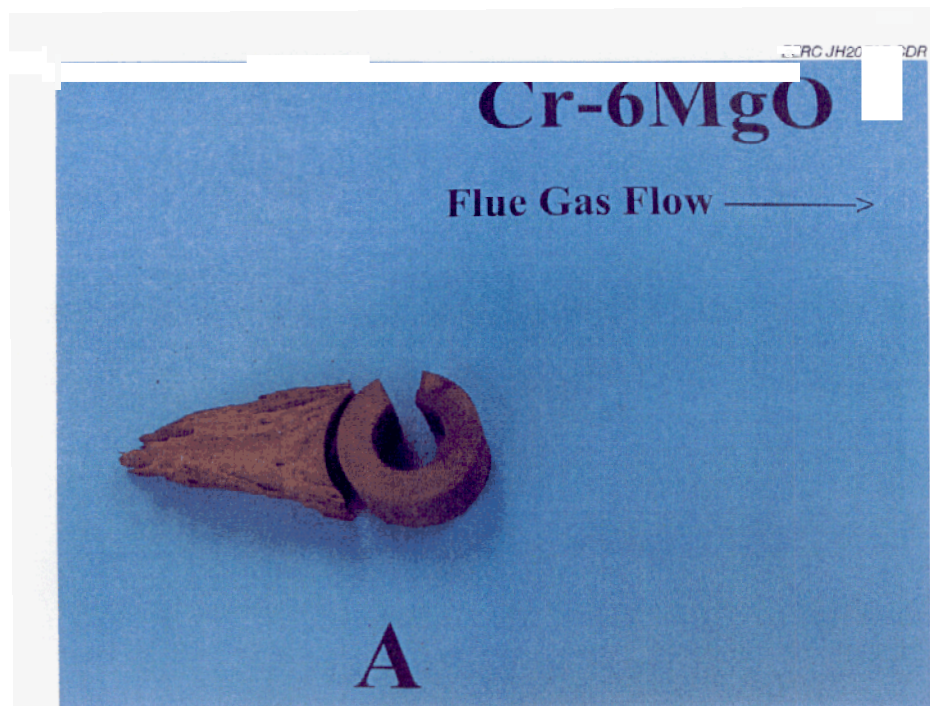


Figure 9. ORNL Cr6-MgO coupon after removal from the SFS.

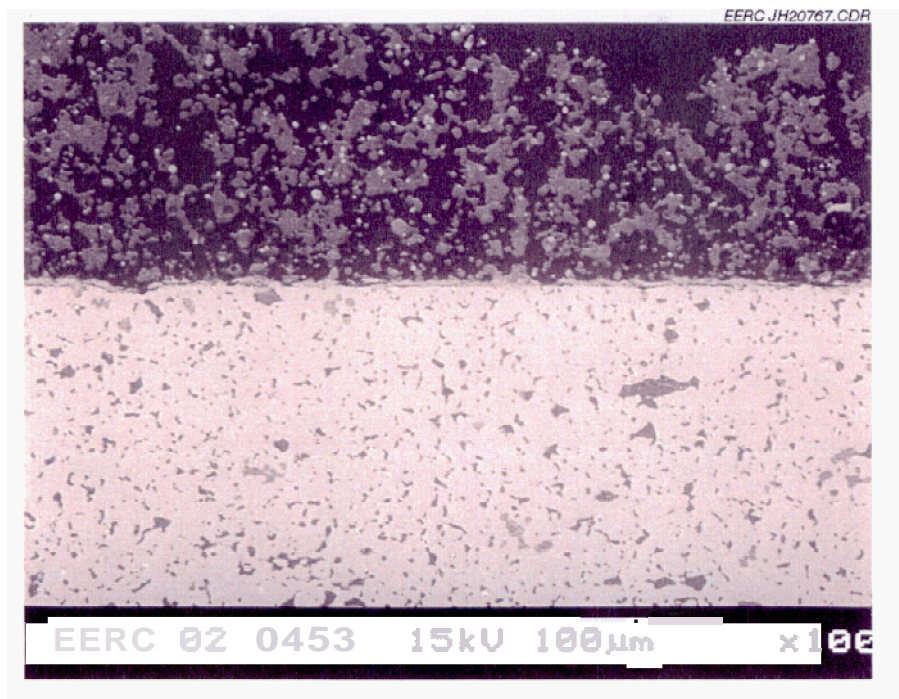


Figure 10. Cross section of alloy at 100x magnification (ORNL Cr6–MgO Coupon A).

The alloy is composed of a chromium matrix with a La-rich phase and a Mg-rich phase. The La-rich phase was analyzed and found to contain 63 wt% La, 22 wt% Ti, 13 wt% Cr, and 2 wt% Mg. The Mg-rich phase was found to contain 21 wt% Mg, 48 wt% Cr, and 31 wt% Ti. Near the surface of the alloy, the lanthanum could only be detected in trace amounts. The Mg-rich phase near the surface was found to lose all but a few percentage of titanium and chromium.

The oxidation layer was irregular in thickness and broken in areas. An average thickness was measured to be 5 μm . The layer also appeared to be poorly attached to the alloy. Figure 11 shows an example of the oxide layer and ash on the alloy at a magnification of 1500x. Iron was found in the oxide layer grading from “not detected” at the alloy interface to as high as 8 wt% at the ash interface. Trace amounts of aluminum and silicon were also detected in the oxidation layer. Chromium was found as high as 5 wt% in the ash above the layer. The ash layer was well adhered to the oxide layer. Evidence of sulfidation or halide attack could not be detected. Oxidation appears to be the corrosion mechanism for this alloy as well, with some interaction of iron from the ash with the oxide layer and some dissolution of the chromia into the ash deposit. Sulfidation, halide attack, or ash constituent interaction directly with the alloy was not detected.



Figure 11. Alloy, oxide layer, and ash deposit at 1500x magnification (ORNL Cr6-MgO Coupon A).

CONCLUSION

All three of the Oak Ridge samples formed a chromia layer on their surfaces. The chromia layers were more bonded to the ash deposit than the alloy and tended to separate from the alloy with the ash deposit leaving only a thin chromia layer behind. The chromia dissolved partially into the deposits and limited amounts of ash constituents dissolved into the chromia layer. This is common for chromia layers formed on other alloy samples analyzed previously. The presence of hollow pores below the layer indicates the loss of alloy material, and the discontinuous nature of the layer further indicates lessened protection to the alloy, although there is much better protection than if no chromium were present. Sulfidation, halide attack, or ash constituent interaction directly with the alloys was not detected.

DISTRIBUTION

ARGONNE NATIONAL LABORATORY
9700 S. Cass Avenue
Argonne, IL 60439
K. Natesan

DOE
DOE OAK RIDGE OPERATIONS
P. O. Box 2008
Building 4500N, MS 6269
Oak Ridge, TN 37831
M. H. Rawlins

DOE
OFFICE OF FOSSIL ENERGY
FE-72
19901 Germantown Road
Germantown, MD 20874-1290
F. M. Glaser

DOE
NATIONAL ENERGY TECHNOLOGY
LABORATORY
626 Cochran's Mill Road
P.O. Box 10940
Pittsburgh, PA 15236-0940
U. S. Rao
R. B. Read
L. A. Ruth

ELECTRIC POWER RESEARCH INSTITUTE
P.O. Box 10412
3412 Hillview Avenue
Palo Alto, CA 94303
W. T. Bakker
J. Stringer

TENNESSEE VALLEY AUTHORITY
Energy Demonstration & Technology
MR 2N58A
Chattanooga, TN 37402-2801
C. M. Huang

WESTINGHOUSE ELECTRIC CORPORATION
Research and Development Center
1310 Beulah Road
Pittsburgh, PA 15235
S. C. Singhal

FOSTER WHEELER DEVELOPMENT
CORPORATION
Materials Technology Department
John Blizard Research Center
12 Peach Tree Hill Road
Livingston, NJ 07039
J. L. Blough

IDAHO NATIONAL ENGINEERING
LABORATORY
P. O. Box 1625
Idaho Falls, ID 83415
R. N. Wright

LEHIGH UNIVERSITY
Materials Science & Engineering
Whitaker Laboratory
5 E. Packer Avenue
Bethlehem, PA 18015
John N. DuPont

NATIONAL MATERIALS ADVISORY BOARD
National Research Council
2101 Constitution Avenue
Washington, DC 20418
K. M. Zwilsky

OAK RIDGE NATIONAL LABORATORY
P.O. Box 2008
Oak Ridge, TN
P. T. Carlson
J. M. Crigger (2 copies)
R. R. Judkins
P. F. Tortorelli
I. G. Wright